Applications of photoswitches in the storage of solar energy

Cai-Li Sun, Chenxu Wang, Roman Boulatov*[a]
[a] Dr. C.-L. Sun, C. Wang and Prof. R. Boulatov
Department of Chemistry, University of Liverpool, Liverpool, L69 7ZD, United Kingdom
E-mail: boulatov@liverpool.ac.uk

Contents

1. Introduction 2
   1.1. Molecular basis of solar thermal energy storage with photoswitches 4
   1.2. The reactions studied for molecular solar thermal energy storage 6
2. Capture of energy 7
   2.1. Matching the dye absorption to the solar spectrum 7
   2.2. Relative and absolute molar absorptivities 10
   2.3. Quantum yield of photoisomerization 11
3. Storage of energy 11
   3.1. Energy density 12
   3.2. Self-discharge rate 16
   3.3. Energy conversion efficiency 17
4. Release of energy 18
   4.1. Power density 18
   4.2. Discharge triggers 18
5. Summary and outlook 19
6. References 20

Photoswitches are organic or organometallic chromophores that undergo a reversible chemical transformation upon absorption of light. Among the most commonly studied photoswitches are stilbenes and azobenzenes, capable of efficient interconversion between *cis* and *trans* isomers. When one isomer is significantly less thermodynamically stable than the other, photoisomerization of the stable to the metastable isomer converts a fraction of the absorbed photon energy into excess free energy (chemical potential). If the metastable isomer is sufficiently inert at room temperature, its photoconversion provides a means of storing solar energy, which is recovered by triggering heat-releasing thermal conversion of the metastable to the stable isomer. In other words, such a photoswitch acts as a battery that captures solar energy, stores it as chemical potential and releases it on demand as heat. This process is known as molecular solar thermal energy storage or a molecular solar thermal battery. Unlike the more established conventional solar thermal storage, which uses sunlight to heat, melt or vaporize material, molecular solar thermal energy storage does not require thermal insulation to prevent discharge but relies on the kinetic activation barrier separating the two isomers. Unlike solar-to-chemical energy conversion by photosplitting of H_2O or photoreduction of CO_2, which comprise open-system cycles, photoswitches are thermodynamically closed storage media. Successful deployment of molecular solar thermal energy storage requires new photoswitches that combine a seemingly contradictory set of molecular parameters: a large difference in the free energies of the two isomers separated by a large kinetic barrier; a high quantum yield of photogeneration of the metastable isomer that itself is either photochemically inactive or transparent to sunlight; highly selective isomerizations that allow many charge/discharge cycles without accumulation of side-products even at high discharge temperatures. While the optimal photoswitch for molecular solar thermal energy storage remains to be invented, a large body of empirical observations acquired in the past decade provides several potentially valuable starting points for such search.

1. Introduction

The importance of solar energy in meeting the ever-increasing energy demands of the human society is well recognized, as is the need for new approaches to its capture, storage and conversion.[1] The already deployed solutions are based on solar thermal and photovoltaic energy conversions.[2] In the former, focused sunlight heats, melts or vaporizes material, with the stored heat later used either directly (e.g., for heating buildings) or is converted to electric current using conventional methods. Photovoltaics converts sunlight directly into electric power. Photocatalytic H_2O splitting to generate H_2 exemplifies conversion of sunlight into chemical potential,[3] a technologically attractive approach that remains confided to labs and small-scale prototypes. A less explored implementation of the same conversion strategy is molecular solar thermal energy storage, also known as molecular solar thermal batteries or solar thermal fuels.

Both implementations of the light-to-chemical-potential conversion strategy exploit photochemistry to drive a thermodynamically unfavourable conversion of a more stable chemical (a reactant) to a less thermodynamically stable one.[4] In both cases, the captured solar energy is recovered in a subsequent exothermic reaction. The key difference between the two implementations is that in molecular solar thermal energy storage neither the capture of energy nor its recovery requires consumption from or release into the environment any additional chemicals. In contrast, photosplitting of H_2O or photoreduction of CO_2 releases O_2, and O_2 is required to convert the captured energy into heat or electric power. This thermodynamically closed operation of molecular solar thermal energy storage, requiring the exchange of only energy, but not matter with its surroundings, engenders this approach with unique advantages but also imposes specific constraints on its chemical implementation. To emphasize these differences we suggest that the term “solar thermal fuels” should not be applied to molecular solar thermal energy storage. Unlike the more established conventional solar thermal (photothermal) energy storage, its molecular solar thermal counterpart requires no thermal insulation as it relies on a kinetic activation barrier to preclude dissipation of the stored free energy and thus potentially allows longer-term energy storage.[5]

The most common chemical implementation of molecular solar thermal energy storage is a pair of isomers, one strained relative to the other. Such isomers belong to a broader category of photochemically active compounds known as molecular photoswitches. Molecular photoswitches undergo a reversible change in molecular geometry, which changes their electronic structure, molecular strain energy and other molecular properties, upon absorption of a photon. Examples of photoswitches include azobenzenes[6] and stilbenes,[7] which interconvert between *cis* and *trans* isomers; norbornadiene/quadricyclane (NBD/QC) derivatives,[8] diarylethenes,[9] and spiropyrans/merocyanines,[10] which undergo reversible electrocyclic reactions and similar concerted pericyclic rearrangements, such as those of dihydroazulene derivatives[11]; and acenes, such as anthracene[12, 13], which photodimerize. Organometallic photoswitches are rarer, one being a fulvalene Ru complex ($FvRu_2$).[14] In all these pairs, one isomer (or the dimer in case of acenes) is thermodynamically less stable than the other. A major thrust of research in molecular photoswitches for molecular solar thermal energy storage is to increase this energy difference without sacrificing the thermal stability of the metastable component or the quantum yield of its photochemical generation.

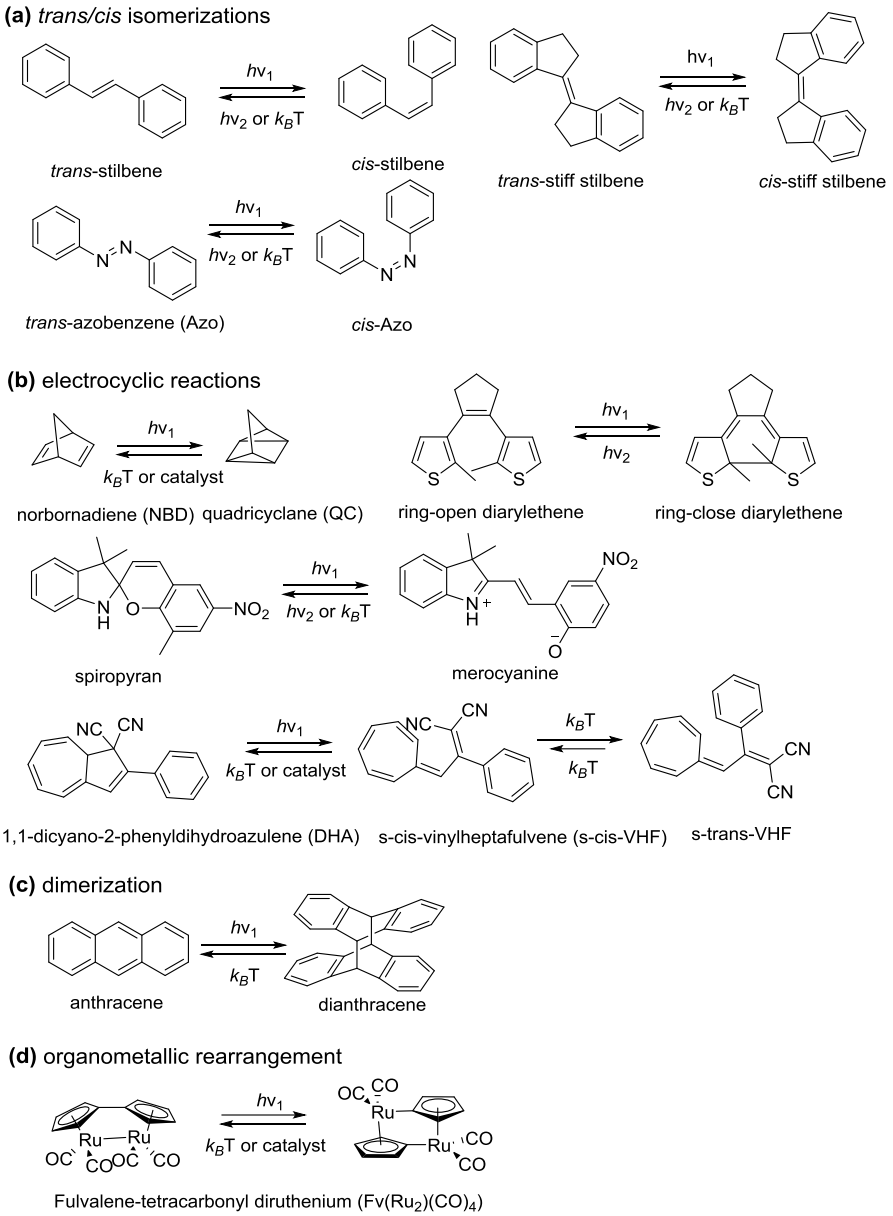

Figure 1. Examples of molecular photoswitches. Only some of these pairs have been studied for molecular solar thermal energy storage, such as trans/cis-stilbene, trans/cis-azobenzene, NBD/QC, DHA/VHF anthracene/dianthracene, and $FvRu_2$ isomers.

The idea of storing solar energy in the form of strained organic molecules was first articulated explicitly in a form that is recognizable today in 1958,[15, 16] which prompted a decade-long burst of activity, followed by dormancy until mid-2000s. Since then the number of published papers in the field has increased every year, but it remains a small fraction of papers devoted to photosplitting of H_2O or photoreduction of CO_2. Various aspects of the field have been reviewed: ref. [17] reviews synthesis and properties of photoswitches for solar thermal energy storage and briefly mentions a few prototype devices; an older review from the same group focuses on molecular design of such photoswitches;[18] studies of azobenzenes only were reviewed in [19] and as an illustration of an application of structured carbon as molecular scaffolds in [20]. Our 2011 review[4] of molecular solar thermal energy storage focused on three areas. First, we proposed broad structure/reactivity trends across all classes of photoswitches suitable for such storage. Second, we defined the fundamental photophysical, thermodynamic and kinetic limits on the key performance characteristics of molecular solar thermal batteries, including energy densities, conversion efficiencies, power outputs, and charging rates.

Finally, we assessed concerns raised in the past about the potential of strained organic molecules to contribute to the mix of technologies for utilization of solar energy.

This review maintains the overall thrust of our 2011 review by focusing on progress towards a deployable solution for solar energy storage using molecular photoswitches. As a result, we organize the discussion below around three broad physical processes that enable molecular solar thermal energy storage: capture, retention and release of energy. To make the review accessible to the broadest audience, we start each section with a brief summary of how each physical process depends on the molecular properties of the photoswitch. The rest of each section compiles and critically assesses the empirical, computational or theoretical results relevant to each step and reported since 2011. Consequently, we discuss all newly reported photoswitches designed for each step together in the corresponding section, irrespectively of their structural similarity or the underlying reaction. Molecules discussed in one section rarely appear in the other sections because their performance in the other steps has not been characterized or is unexceptional, illustrating the paucity of work that takes a systems approach to the problem of designing the optimal photoswitch.

The field continued to evolve along the broadly similar trends identified in the 2011 review. Synthetic effort focused primarily on optimizing the existing photoswitches for improved performance in either capture, retention, or release of energy. For example, the majority of recently reported derivatives of NBD (Figure 1) were designed to absorb at longer wavelengths than the parent, with the goal of improving the fraction of solar flux that they can capture. The reported work on azobenzenes has been dominated by attempts to immobilize various derivatives on structured carbon support or in polymer networks to increase the activation or standard free energies of *cis*→*trans* isomerization, which improves energy release. In terms of the underlying reaction, the largest volume of work in the field of solar thermal energy storage in the past 10 years has been on NBD isomerization, followed by azobenzenes. Publications on the derivatives of the DHA or $FvRu_2$ photoswitches are limited and mostly focus on improving syntheses or on computations of properties. Device design and engineering have received comparably less attention.

To maintain the scope of the review manageable and to avoid duplicating the existing reviews, we avoid discussing synthetic methodology, as important as it is in yielding the desired photoswitches, and mention molecular design only when it illustrates broader trends in how molecular structure may be exploited to improve a physical component of the energy storage cycle.

1.1. Molecular basis of solar thermal energy storage with photoswitches

Recharging a molecular solar thermal battery starts with absorption of a photon by the stable isomer, which causes the vertical electronic transition from the singlet ground state (S_0) of the chromophore to its first singlet excited state (S_1). Fast relaxation of this Franck-Condon configuration through the minimum energy conical intersection (MECI) of S_0/S_1 seam returns the molecule to its ground electronic state, where it continues to change its geometry to yield either the metastable product, or revert to the reactant. The battery is discharged when an external trigger (such as localized transient heating or exposure to catalyst) causes the metastable product to revert to the stable isomer over an activation barrier on the S_0 surface with release of heat. The free energy of this reversion ($-\Delta G_{isom}$) defines the upper limit of thermal energy that can be stored per mole of the chromophore; its activation free energy ($\Delta G_{rev}^{\neq}$) determines the self-discharge rate of the battery at the storage temperature. Because of the low reaction and activation entropies of many isomerization reactions, the thermodynamics and kinetics of the reactions are often quantified by enthalpies, ΔH_{isom} and $\Delta H_{rev}^{\neq}$ instead of free energies; a fraction of papers in the field use these thermodynamic functions interchangeably.

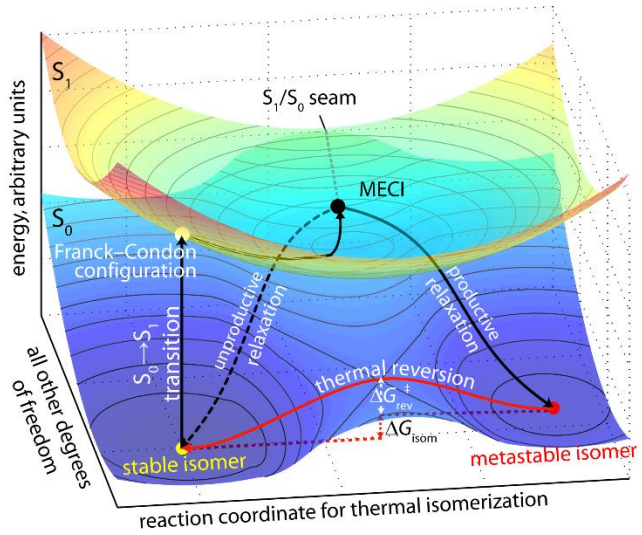

Figure 2. A schematic representation of the energy surfaces underlying thermochemical energy storage. Reproduced with permission from Ref. [4]. Copyright (2011) The Royal Society of Chemistry.

A practical utility of a molecular solar thermal battery is likely determined by at least (i) charging rate under ambient solar light; (ii) maximum achievable energy and power densities; (iii) self-discharge rate; (iv) ease of inducing discharge and controlling its rate; (v) the number of charge/recharge cycles (cyclability); (vi) cost. Achieving useful values of these parameters requires designing dyes to maximize (i) visible-light photochromism, i.e., the difference in absorptivities of the stable and metastable forms in the 350 – 600 nm range, corresponding to the maximum intensity of solar radiation; (ii) the quantum yield of photoisomerization of the stable to the metastable isomer, i.e., the probability that the photoexcited stable isomer will isomerize, φ_{isom}; (iii) the free energy difference between the two forms, ΔG_{isom}; (iv) the activation free energy of thermal relaxation of the metastable isomer, $\Delta G_{rev}^{\neq}$; and minimize (v) its molar mass, MM and (vi) photo- and thermal side reactions that may accompany isomerizations. Some of these parameters are fundamentally coupled: for example, shifting the absorption maxima to longer wavelengths requires increasing conjugation, and correspondingly the MM. Increasing the wavelength capable of affecting photoisomerization or increasing the energy difference between the two isomers, ΔG_{isom}, usually decreases the activation barrier of thermal relaxation, $\Delta G_{rev}^{\neq}$.

These parameters affect the performance characteristics of a battery nonlinearly. For example, the maximum achievable energy density, ED, of a battery is determined both by ΔG_{isom} and the composition of the photostationary state, which reflects the maximum fraction of the stable isomer that can be photoisomerized to the metastable analog. Small ΔG_{isom} decreases both the energy density and the conversion efficiency (the fraction of absorbed photon that is converted to chemical potential and is stored), and may require sophisticated heat management of a charging battery as most of the absorbed light simply heats the battery. The composition of the photostationary state depends on the product of the ratios of the quantum yields of productive (stable -> metastable isomer, φ_{isom}) to unproductive (metastable -> stable isomer, φ_{rev}) isomerizations and of the extinction coefficients of the stable and metastable isomers, respectively, averaged over the irradiation wavelengths. Full conversion of the stable to the metastable isomers would require either $\varphi_{isom} = 1$ or if $\varphi_{isom} < 1$ the metastable isomer being transparent at all irradiation wavelength. Photoisomerizations with unit quantum yields are quite rare, and to the best of our knowledge no molecular design principles have been articulated to systematically increase the quantum yield of isomerization. Thus, a practical approach to maximizing the energy density is to maximize the degree of photochromism while maintaining the extinction coefficient (ε_{max}) of the stable isomer at the wavelength of the maximum-intensity radiation above ~(10 $mol^{-1}cm^2$)MM, which corresponds to absorption of 90% of incident radiation by an mm-thick layer of a hypothetical dye of molar mass MM and density of 1 g/mL. These

values are derived from the Beer-Lambert law, $\log(I_0/I) = \varepsilon_{max}bc$: to get 90% absorbance ($I_o/I = 10$) by a 1-mm thick layer (b = 0.1 cm) of neat dye with density of 1 g/mL (corresponding to concentration, c, of density/molar mass, or 1/MM) requires an extinction coefficient, $\varepsilon_{max} = \log(I_0/I)/bc = 10MM$ where MM is in g/mol and ε_{max} in $M^{-1}cm^{-1}$.

1.2. The reactions studied for molecular solar thermal energy storage

An optimal photoswitch for molecular solar thermal energy storage remains to be designed and synthesized. The current reported effort to do so mainly focuses on improving one of the 4 pairs of photoswitches in Figure 1 by peripheral substitution. The parameters of these 4 pairs that determine its photochemistry (e.g., quantum yields) and its thermal chemistry (activation and standard energies) form the dataset against which current progress towards an optimal molecule for molecular solar thermal energy storage can be assessed.

The NBD/QC pair, which was the main subject of extensive early work in the field,[8, 21] is the only reaction known to date theoretically capable of yielding a battery with the maximum energy density approaching the fundamental upper limit for a solar thermal battery of ~1 MJ/kg[4], thanks to the high standard enthalpy of reversion of QC to NBD (ΔH_{isom}= 89 kJ/mol)[22] and the low MM of 92 g/mol. QC is stable at room temperature (half-life, $t_{½}$, ~10^7 h at 300 K),[23] but the absorption spectrum of NBD, which is confined to wavelengths <267 nm, does not overlap with the solar spectrum, which starts at ~340 nm[24]. As a result, a battery utilizing unsubstituted NBD/QC cannot be recharged by ambient sunlight.

Table 1 Key paprameters of the four reaction pairs used in most research on solar thermal energy storage. See Figure 1 for molecular structures.

photoswitch	$\lambda_{max,s}$, nm*	φ_{isom}	$\lambda_{max,m}$, nm*	ΔH_{isom} or ΔG_{isom}, kJ/mol	$\Delta H_{rev}^{\neq}$ or $\Delta G_{rev}^{\neq}$, kJ/mol	MM, g/mol
NBD/QC	213, 236[25]	~0.05[8]	<210	89±1[22]	140[23]	92
trans/*cis*-azobenzene	~320[6]	0.10-0.35[6]	~450[6]	49±5[26]	95[27]	182
DHA/VHF	~350[28]	0.35-0.55[29]	~470[28]	~28** [30]	106^[31]	256
$FvRu_2$	~350[32]	0.13-0.17[32]	?	83±6[33]	125±8[33]	444

* $\lambda_{max,s}$: the maximum absorptive wavelength of stable isomer; $\lambda_{max,s}$: the maximum absorptive wavelength of metastable isomer.
**The free energy difference between s-*trans*-VHF and DHA.
^ The activation free energy of s-*cis*-VHF to DHA.

Azobenzene is moderately photochromic with the absorption spectra of both isomers overlapping with the solar spectrum; azobenzene and many of its derivatives manifest high photostability, necessary for high cyclability. However, the azobenzene core is conformationally flexible, significantly limiting the opportunities to increase the energy difference between the two isomers by means of molecular design. With very few exceptions,[34, 35] even strain-free *cis* azobenzenes revert to the *trans* isomer with half-lives of hours at room temperature.

1,1-dicyano-2-phenyldihydroazulene, which confusingly is referred in the literature on photoswitches simply as dihydroazulene, DHA, is a rare example of a unidirectional photoswitch. The product of its photoisomerization, a heptafulvene derivative colloquially named VHF (for vinylheptafulvene) is not photochemically active. The molecular origin of the unidirectionality is not fully understood, but is thought to result from the relaxation of Frank-Condon DHA into s-*cis*-VHF, which rapidly relaxes to s-*trans*-VHF. Photoexcited s-*trans*-VHF relaxes through the same s-*cis*-VHF geometry and hence cannot reach DHA. VHF is thermally moderately stable ($t_{½}$ ~ 88 h at 300 K)[11, 30] and both isomers are compatible with high cyclability.[36] However, s-*trans*-VHF is only 28 kJ/mol[30] less stable than DHA, corresponding to a low maximum energy density and conversion efficiency: ΔG_{isom} alone limits the

fraction of the absorbed photon energy converted to the excess chemical potential of VHF to 8%, the rest being lost as heat.

$FvRu_2$ absorbs at the wavelengths close to the maximum of the solar spectrum, producing a thermally stable isomer ($t_{½}$ ~10^5 h at 300 K, $\Delta H_{rev}^{\neq}$ = 125±8 kJ/mol) [33] with ΔH_{isom} = 83±6 kJ/mol[32, 37]. Despite the effort devoted to its molecular modifications[38-40] and integrating it with upconversion [41], the high molar mass and cost of Ru probably make $FvRu_2$ suboptimal for practical molecular solar thermal energy storage.

2. Capture of energy

2.1. Matching the dye absorption to the solar spectrum

Intensity of solar radiation with wavelengths shorter than ~340 nm is probably too low at the Earth surface to be of practical uses for molecular solar thermal energy storage.[42] The photon energy decreases inversely with its wavelength and given the fundamental limits on the fraction of absorbed photon energy that can be converted to chemical potential in a closed system, and the importance of high energy density in any practical energy storage solution, solar radiation with wavelengths above ~500 nm seems unlikely to be utilizable for practical molecular solar thermal energy storage. Consequently, a perfectly optimized dye for such applications should undergo photoisomerization on absorption of light in the 350-450 nm range.

Among the 4 motifs in Table 1, only NBD is transparent in this window and considerable effort has been invested in varying peripheral substitution of NBD to shift its absorption to higher wavelengths while minimizing the necessary increase in the molecular weight.[8, 24, 43-51] The resulting large amount of experimental and computed data on the dependence of the absorption maxima, and reaction and activation free energies on the substituents illustrate the complexities of balancing the often opposing effects of such substituents on these molecular parameters. Two approaches, potentially applicable to other promising candidates for molecular solar thermal energy storage emerge from this compilation. One is pairing of an electron-withdrawing and electron-donating substituent to create so-called push-pull effect, which red-shifted the NBD absorption maxima by up to 170 nm (Figure 3). The other is to minimize the inevitable increase in the molecular weight of such substitution by linking two or three CN-substituted NBD chromophores by a single electron-rich aromatic moiety. A fortunate if unexpected side-effect of this linking was the emergence of cooperativity in some (but not all) NBD dimers. The activation energies of thermal isomerization of each QC moiety in **29** and **31** depended on the isomeric state of the other moiety: QC,QC->NBD,QC isomerization was slower than the QC,NBD->NBD,NBD analog (Figure 4).[50] The molecular origin of this cooperativity, which is probably electronic, remains to be understood, as is the likelihood that the same approach can be applied to other chromophores.

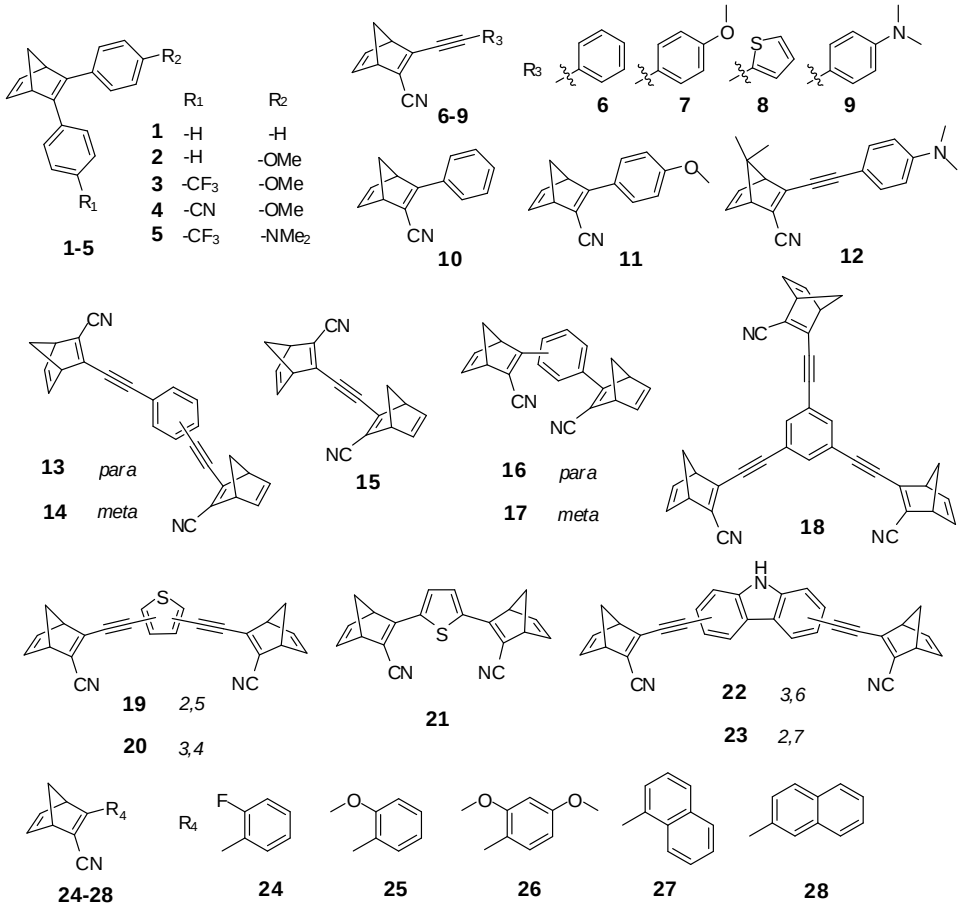

Figure 3 Examples of NBD derivatives with absorption maxima within the range of solar radiation on Earth.

These gains in spectral overlap, however, came at a cost. First, photoisomerization of a single NBD chromophore in NBD dimers **15**-**16** shifted the maximum absorption of the remaining NBD chromophore to shorter wavelength by ~50 nm, or half the difference between all-NBD isomer of **15**-**16** and unsubstituted NBD. The absorption spectra of the other multi-NBD chromophores in mixed-isomer states have not been reported. Since mixed-isomer NBD,QC pairs are more thermally labile than the QC,QC isomers, NBD dimers/trimer are practical only if all NBD moieties are converted to QC, which requires irradiation at shorter wavelength that the absorption spectrum of the all-NBD isomer. Second, electron-donating aromatic substituents that red-shift NBD absorption the most also increase the spectral overlap of the NBD and QC-containing isomers, which is especially pronounced in **23**. A similar phenomenon was observed[52, 53] in the DHA photoswitches: substituents that red-shift the absorption maximum of DHA also increase the spectral overlap of the isomers, which is already present in the unsubstituted derivatives.[11] Unlike QC, VHF does not photoisomerize, somewhat mitigating the impact of this undesired spectral overlap on the performance of the modified DHA photoswitches. The similar absorption spectra of derivatives **24**-**28**,[48] containing increasingly electron-rich phenyl substituent, suggest that the extent of the π-system, rather than the electron-donating properties of the aromatic group are the main determinants of the absorption maxima of the NBD chromophore.

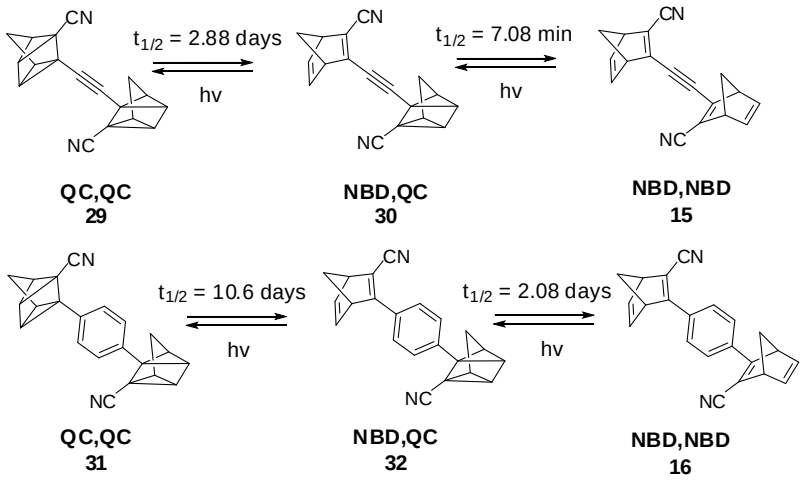

*Figure 4 Stepwise conversion of QC dimers **29**, **31** to NBD dimers **15**, **16**. Half-lives of **29**-**32** from Ref. [50]*

The summary of the correlations of maximum absorption wavelength, λ_{max}, energy density, ED, and the activation barrier for QC→NBD isomerization, $\Delta G_{rev}^{\neq}$, (Figure 5) illustrates how hard it is to improve the NBD photoswitch. The most-optimized peripheral substitution shifts the absorption of the NBD dye by up to ~100 nm per 100 g/mol increase in the MM, while inevitably decreasing $\Delta G_{rev}^{\neq}$ and the energy density. Sacrificing 20-30 kJ/mol of $\Delta G_{rev}^{\neq}$ to improve the overlap of the absorption spectrum with that of solar radiation does not diminish the suitability of the NBD core for molecular solar thermal energy storage, but the concomitant decrease in the energy density does: note that the highest ED of the substituted NBDs is almost 45% lower than that of unsubstituted NBD.

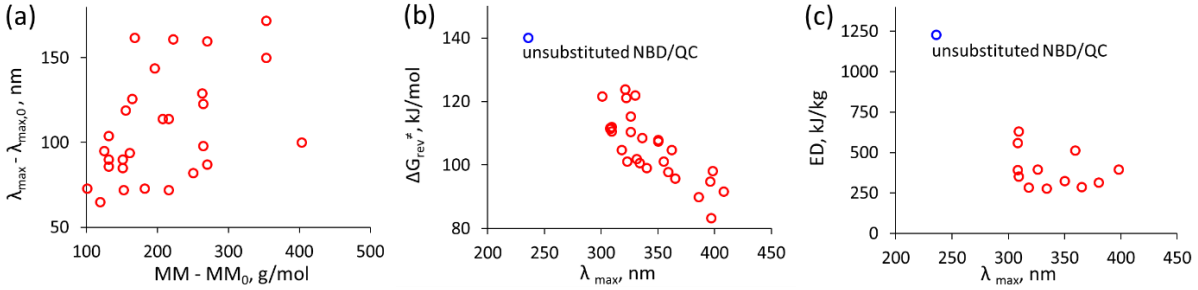

Figure 5 Correlations of the maximum-absorption wavelength, λ_{max}, molecular mass, MM, activation barrier, $\Delta G_{rev}^{\neq}$, and energy density, ED, of NBD derivatives. (a) The increment of maximum-absorption wavelength of substituted NBDs relative to unsubstituted NBD ($\lambda_{max} - \lambda_{max,0}$) vs. the difference of their molar masses ($MM - MM_0$). (b) The activation barrier vs. λ_{max}. (c) The energy density vs. λ_{max}. The blue points in (b) and (c) are those for unsubstituted NBD. The plotted data are listed in Table 2.

Table 2. Molar mass (MM), λ_{max}, half-life ($t_{1/2}$), activation free energy of thermal isomerization ($\Delta G_{rev}^{\neq}$), the absolute value of the enthalpy of isomerization (ΔH_{isom}) and energy density (ED) of NBD derivatives shown in Figure 3.

	MM, g/mol	λ_{max}, nm	$t_{1/2}$, h (25 °C)	$\Delta G_{rev}^{\neq}$, kJ/mol	ΔH_{isom}, kJ/mol	ED, kJ/kg
NBD	92	236	~10^7	140	113	1228
1[24]	244	308	1030	111	96	393
2[24]	274	309	751	111	97	354
3[24]	342	318	70	105	98	287
4[24]	299	350	209	107	97	324
5[24]	355	365	1.9	96	102	287
6[44]	217	331	22	102	--	--
7[44]	247	355	16	101	--	--

8[44]	223	340	7.4	99	--	--
9[44]	260	398	5	98	103	396
10[44]	193	309	1320	112	122	632
11[49]	223	326	720	111	89	397
12[47]	288	380	--	--	91	315
13[50]	356	359	4.3*	98	183	514
14[50]	356	334	14*	101	99	278
15[50]	256	362	69*	105	--	--
16[50]	308	350	254*	108	--	--
17[50]	308	308	1164*	112	173	562
18[50]	495	336	317*	108	--	--
19[51]	362	396	1.32*	95	--	--
20[51]	362	323	16.1*	101	--	--
21[51]	314	397	0.01*	83	--	--
22[51]	445	386	0.18*	90	--	--
23[51]	445	408, 397	0.37*	92	--	--
24[48]	211	301	64320	122	--	--
25[48]	223	322	54552	121	--	--
26[48]	253	330	71304	122	--	--
27[48]	243	321	161496	124	--	--
28[48]	243	326	5088	115	--	--

* The half-life for QC/QC->NBD/QC or QC/QC/QC->NBD/QC/QC isomerizations.

Since all other photoswitches in Table 1 absorb in the 350 – 450 nm range, tuning their absorption spectra by peripheral substitution has attracted comparably little effort in context of molecular solar thermal energy storage.

2.2. Relative and absolute molar absorptivities

An ideal metastable isomer should be transparent at the wavelengths used to charge a solar battery. The optimal value of the molar absorptivity of the stable isomer depends on how this charging is implemented technically. The more absorbing the material, the thinner its layer at the transparent surface of the battery within which all incident solar radiation is absorbed. Even an ideal chromophore with a unit quantum yield of photoisomerization to the metastable isomer, converts a major fraction of the absorbed light into heat. Depending on the photon flux, a highly absorbing medium may produce thermal fluxes that would require active cooling to prevent the local temperature from increasing to a value where the metastable isomer becomes unstable on the charging timescale (this waste heat can still be utilized[54]). Both push-pull substituents and extended π-conjugation increase the extinction coefficient,[55] which was exploited to increase the maximum extinction coefficients of NBD derivatives **6**-**9** by 2-4 times relative to that of **10** but it remains to be understood whether absorptivities of the other chromophores in Table 1 are comparably sensitive to similar structural modifications.[44]

With the exception of QC, all other metastable isomers in Table 1 absorb in the 350 – 450 nm range. This absorption affects the battery performance in three ways. First, it increases the thermal flux that need to be managed during charging. Second, it decreases the incident radiation flux reaching the stable isomer. Third, it decreases the fraction of the metastable isomer at the photostationary state (the inability of VHF to photoisomerize eliminates the last effect for the DHA photoswitch). One potential solution is to increase photochromicity of a pair of isomers, by modifying absorptivities of the two isomers independently. So far, such independent tuning of absorption spectra has been

difficult. Examples of NBD and DHA derivatives demonstrate that substituents change absorptivities of the two isomers in the same manner: either increasing or decreasing both at most wavelengths.

An alternative approach of suppressing light absorption by the metastable isomer through device engineering instead of molecular design was reported[56] but whether it results in the net gain of performance remains to be determined. The reported prototype combined two layers of azobenzene derivatives (with λ_{max} = 323 nm and 460 nm, λ_{max} = 351 nm), and two filtering layers, one comprising a coumarin fluorophore, the other being a bandpass filter. The logic of using an additional coumarin layer is unclear, because its emission spectrum appears to overlap equally well with the long-wavelength portion of the absorption spectra of both isomers, thus not affecting the composition of the photostationary state. Both layers contribute to the mass (and complexity) of the device without storing energy.

2.3. Quantum yield of photoisomerization

Most photoisomerizations proceed with quantum yields, $\varphi_{isom}<1$. If the metastable isomer is either transparent at the irradiation wavelength, photochemically inert (like VHF), or both, $\varphi_{isom}<1$ lowers the fraction of absorbed radiation that is converted into chemical potential. It doesn't affect the energy density because the photostationary state can still be driven arbitrarily close to containing only the metastable isomer, albeit at increasingly long irradiation times (or higher photon fluxes) as φ_{isom} decreases to 0. The absorption spectra of both isomers of most candidates for molecular solar thermal energy storage partially overlap, making it impractical or impossible to limit incident light only to the wavelengths where the metastable isomer is transparent. Likewise, with the exception of the DHA photoswitch, whose metastable isomer (VHF) does not photoisomerize, both isomers are photochemically active, i.e., each photoisomerizes into the other with some probability. As a result, irradiating either isomer or a mixture of isomers of an arbitrary composition eventually produces a photostationary state whose composition does not change upon continued irradiation. If both isomers are thermally stable, the ratio of their molar fractions at the photostationary state, χ_1/χ_2 equals the inverse of the product of the ratios of their extinction coefficients ($\varepsilon_1/\varepsilon_2$) and isomerization quantum yields ($\varphi_{1\text{->}2}/\varphi_{2\text{->}1}$) because $\chi_1/\chi_2 = k_2/k_1 = \varepsilon_2\varphi_{2\rightarrow1}/(\varepsilon_1\varphi_{1\rightarrow2})$, where k is a photochemical isomerization rate constant. The more absorbing the isomer is or the higher the quantum yield of its photoisomerization is the smaller its fraction in the photostationary state.

Few general rules have been identify to predict how a quantum yield of isomerization is affected by substituents, the molecular strain of the isomers,[57] or the polarity of the solvent, although for individual chromophores (e.g., azobenzenes[6] or DHA[11]) a few empirical trends are known. This fact contrasts with a well understood relationship between the effective viscosity of the surroundings and the quantum yield of isomerization, which has been extensively exploited to increase fluorescence quantum yields (at the expense of isomerization) of otherwise weakly fluorophoric dyes. An exception is photoisomerization of $FvRu_2$ which reflects kinetic competition between thermally-activated processes in the S_0 state and thus is more amenable to systematic improvement by substitution that affect the relevant activation barriers.[40] A recent computational study attempting to rationalize the geometry of the minimum-energy conical intersection is a tentative step towards being able to affect quantum yields of isomerizations by controlling the molecular geometry of the conical intersections through the dye substitution pattern.[58]

3. Storage of energy

Molecular properties of the isomer pair directly affect two performance characteristics of molecular solar thermal energy storage: maximum achievable energy density, which increases linearly with ΔG_{isom} and self-discharge rate, with decreases exponentially with $\Delta G_{rev}^{\neq}$ (Figure 2). A photon of 340 nm, the lowest-wavelength solar radiation with useful intensity at Earth surface, is ~350 kJ/mol. Only a fraction of this energy can be stored as chemical potential. The simplified potential energy surface diagram in Figure 2 demonstrates that the energy of the absorbed photon always exceeds the sum $\Delta G_{isom} + \Delta G_{rev}^{\neq}$ (see Figure 2 for the relationship between ΔG_{isom} and $\Delta G_{rev}^{\neq}$). Empirical data suggest

that ΔG_{isom} rarely if ever exceeds $\Delta G_{rev}^{\neq}$ in strained organic molecules. As a result, the fundamental limit on ΔG_{isom} for any given $\Delta G_{rev}^{\neq}$ and λ_{max} likely exists but is unknown. A broad relationship between ΔG_{isom}, $\Delta G_{rev}^{\neq}$, λ_{max} and φ_{isom} also seems plausible. For all reactions in Table 1, both ΔG_{isom} and $\Delta G_{rev}^{\neq}$ are in theory amenable to tuning by molecular design, if not necessarily independently, although in practice the results have been mixed, as detailed below.

3.1. Energy density

Volumetric and gravimetric energy densities are key parameters that define the utility of a battery. For molecular solar thermal energy storage, volumetric densities are generally high because the material is a liquid or a solid in both isomeric states and hence occupies a small molar volume. The gravimetric energy density, ED, correlates positively with ΔG_{isom} (Figure 2: remember that $\Delta G_{isom} \sim \Delta H_{isom}$ because the entropy change in isomerizations is typically small); the molar fraction of the metastable isomer at the photostationary state, χ_m; and the mass fraction of the photoswitch in the material, w_p; but correlates negatively with the molar mass of the photoswitch:

$$\mathrm{ED} = \frac{\Delta \mathrm{H}_{\mathrm{isom}} \chi_m \mathrm{w}_p}{\mathrm{MM}}$$

The most common strategy of increasing ED is to increase ΔG_{isom} usually by increasing the molecular strain of the metastable isomer either through molecular architectures or molecular packing. So far the application of either strategy to molecular solar thermal energy storage has produced mixed results.

Incorporating stiff stilbene in a macrocycle (Figure 6) was used successfully in several studies to systematically vary the strain energy of its *trans* isomer, relative to the *cis* analog, in ~10-15 kJ/mol increments up to ~130 kJ/mol.[59-66] Whereas the capacity of stiff stilbene to accommodate large molecular strains has been exploited to build molecular motors[67] and in photocontrol of catalysis,[68] stiff stilbenes have not yet been studied for molecular solar energy storage. However, initial attempts to incorporate other photoswitches into macrocycles have been reported. The conformational flexibility of both azobenzenes and VHF presents considerable barrier to such effort. For example, a computational study[69] suggesting that even doubling ΔG_{isom} of azobenzene requires simple-looking but synthetically inaccessible azobenzene macrocycles.

Application of macrocyclization strategy to increase ΔG_{isom} of the DHA photoswitch has so far been unsuccessful. In the three homologous macrocyclic derivatives, the DHA,DHA isomers **33**-**35**,[71, 72] were calculated to be 3-5 kJ/mol less stable than the mixed DHA,*trans*-VHF analogs **36**-**38** whereas in the acyclic parent DHA/VHF pair (Figure 1) VHF's free energy is ~28 kJ/mol above that of the DHA isomer. However, the observed thermal relaxation of mixed DHA,VHF isomers **36**-**38** to the DHA,DHA analogs **33**-**35** requires that the DHA,DHA isomer be more stable than the DHA,VHF analog, contradicting the computational results. In only one VHF,VHF macrocycle, **40**, was the minimum-energy isomer identified computationally as s-*cis*/s-*cis* (the other isomers of bis-heptafulvene macrocycle are *cis*/*trans* and *trans*/*trans*), which was calculated to be only 28 kJ/mol less stable than the DHA dimer, or half ΔH_{isom} of parent VHF. In other words, the design of macrocycles **33**-**41** strained the DHA and *trans*-VHF forms more than it did the *cis*-VHF isomer. In all three macrocycles the VHF,VHF form **39**-**41** was considerably more labile ($t_{½}$ ~ 1 h) then parent acyclic VHF whereas in the DHA,VHF macrocycles the thermal stabilities of the VHF isomer were comparable to those of parent acyclic VHF ($t_{½}$ ~100 h). Unlike QC dimers **29** and **31**, the two reactive sites of **33**-**35** did not manifest cooperativity. Photochemical properties of macrocycles **33**-**41** have not been reported.

The data above suggest that a successful application of the macrocyclization strategy to the DHA photoswitch would likely require an approach similar to that successfully applied to the design of reactive sites whose kinetic stability is affected by tensile load.[73-76] For the DHA photoswitch, this approach requires calculations of the difference of each non-bonding internuclear distance between the three isomers: DHA, *cis*-VHF and *trans*-VHF to identify the pair(s) of atoms that move farther apart

upon conversion of DHA to either isomer of VHF. The pair experiencing the largest elongation should be bridged by a molecular linker long and flexible enough to remain largely strain-free in the DHA isomer but is too short to accommodate the increased internuclear distance of the (preferably cis) VHF isomer.

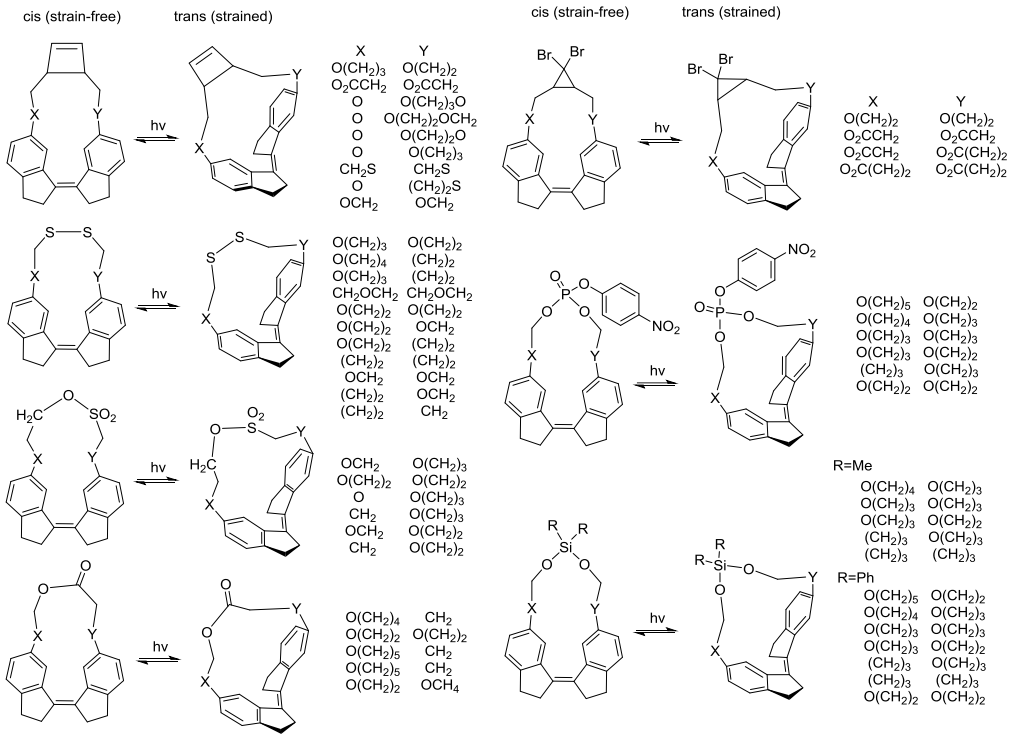

Figure 6. Examples of stiff-stilbene macrocycles which allow gradual tuning of ΔG_{isom} from ~-10 kJ/mol in free cis/trans stiff stilbene[70] to ~130 kJ/mol for the smallest macrocycle.

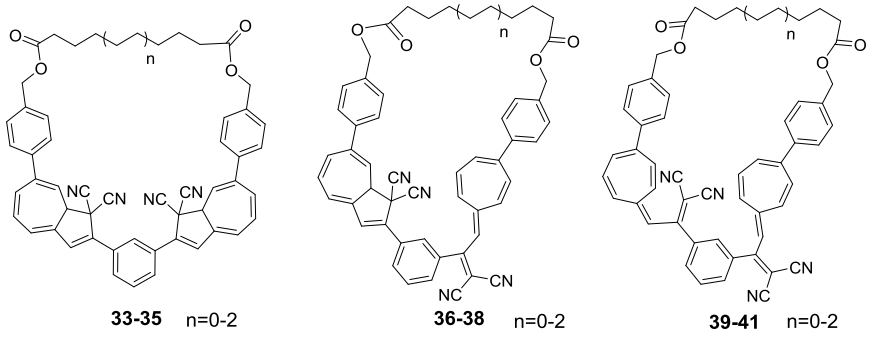

Figure 7. The three isomers of the only macrocyclic derivatives of the DHA photoswitch reported to date.

Few examples have been reported of using bulky substituents to increase ΔG_{isom} (Figure 8): for example, ΔG_{isom} of azobenzene derivatives **42**-**44** is 30-40 kJ/mol higher than that of unsubstituted azobenzene due to steric repulsion of the phenyl substituents in the *cis* isomer.[77] Conversely, introducing bulky substituted in the NBD core (**45**-**47**) decreased ΔG_{isom} by 4-43 kJ/mol.[47] Similarly, ΔG_{isom} of 1,1-dicyano-2-phenyldihydroazulene, DHA is half that for mono-cyano analog, **48** (28 vs. 58 kJ/mol, according to DFT calculations), which was attributed to elimination of excess steric strain of the doubly substituted fused five-membered ring.[30] C3-substitution of the DHA core, **49**, is also effective, nearly doubling ΔG_{isom} of parent DHA.[52] Surprisingly, 3-phenyl derivative of **48** (mono-cyano dihydroazulene) has not been reported even though group additivity suggests that its ΔG_{isom} may reach a practically useful value of >80 kJ/mol. Because the effect of bulky substituents on isomerization energies of simple organic molecules is reasonably amenable to DFT calculations with conventional

functions (e.g., B3LYP), a systematic computational optimization of the substitution patterns of isomer pairs in Table 1 to maximize ΔG_{isom} seems likely to be productive.

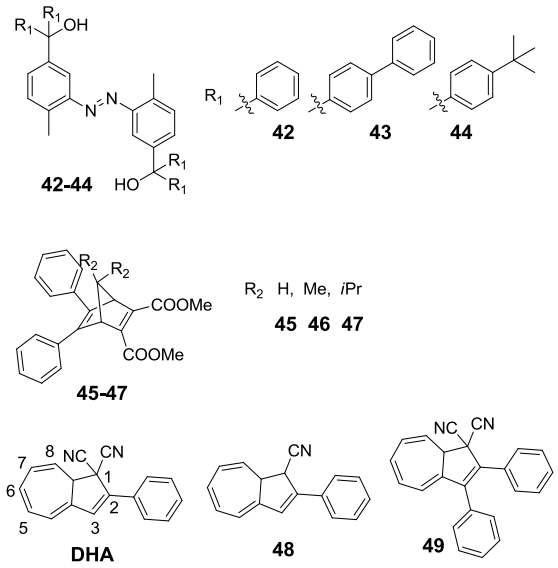

Figure 8. Reported derivatives of azobenzene, NBD and DHA bearing bulky substituents.

Attempts to exploit the different intermolecular packing of the stable and metastable isomers to increase the energy density of a battery have been reported. In this approach, individual chromophores no longer react independently, but rather a domain of thousands or more molecules undergoes cooperative isomerization, resembling a phase transition. A similar approach has been exploited successfully in photoactuating liquid crystals.[78] To date realization of this idea required binding azobenzene derivatives to single-walled carbon nanotubes (SWCNT),[27, 79] other structured carbon, such as reduced graphene oxide (RGO)[80-85] or polymers, such as polymethylacrylate, PMA (Figure 9, Table 3).[86-88] Such hybrid materials typically have energy densities below that of unsubstituted azobenzene, reflecting the extra mass of the non-energy storing matrix. Increased energy densities compared to unsubstituted azobenzene were claimed in several cases, but the highest values had been derived from differential-scanning-calorimetry (DSC) traces that correspond to negative heat capacities, suggesting potential instrumental artifacts, or seem to be inconsistent with the raw data cited in support of such claims. We suggest that these high EDs should be considered tentative until confirmed. These aggregates generally increase the half-life of the *cis* isomer but the magnitude is comparable to that achievable by peripheral substitution.

Qualitatively, the molecular origin of increased ΔH_{isom} in such aggregates is probably destabilization of one isomer surrounded by the molecules in the other isomeric state compared to the same isomer surrounded by the molecules in the same isomeric state. However, the effect of this aggregation on the quantum yields and the compositions of the photostationary states have not been fully quantified. Whether or under what circumstances the EDs and/or $\Delta G_{rev}^{\neq}$ values of the scale unambiguously demonstrated so far with this approach justify the extra costs of the material has not yet been discussed in the literature. Likewise, the performance impact of the increased background absorbance and the increased complexity of device fabrication remains to be addressed.

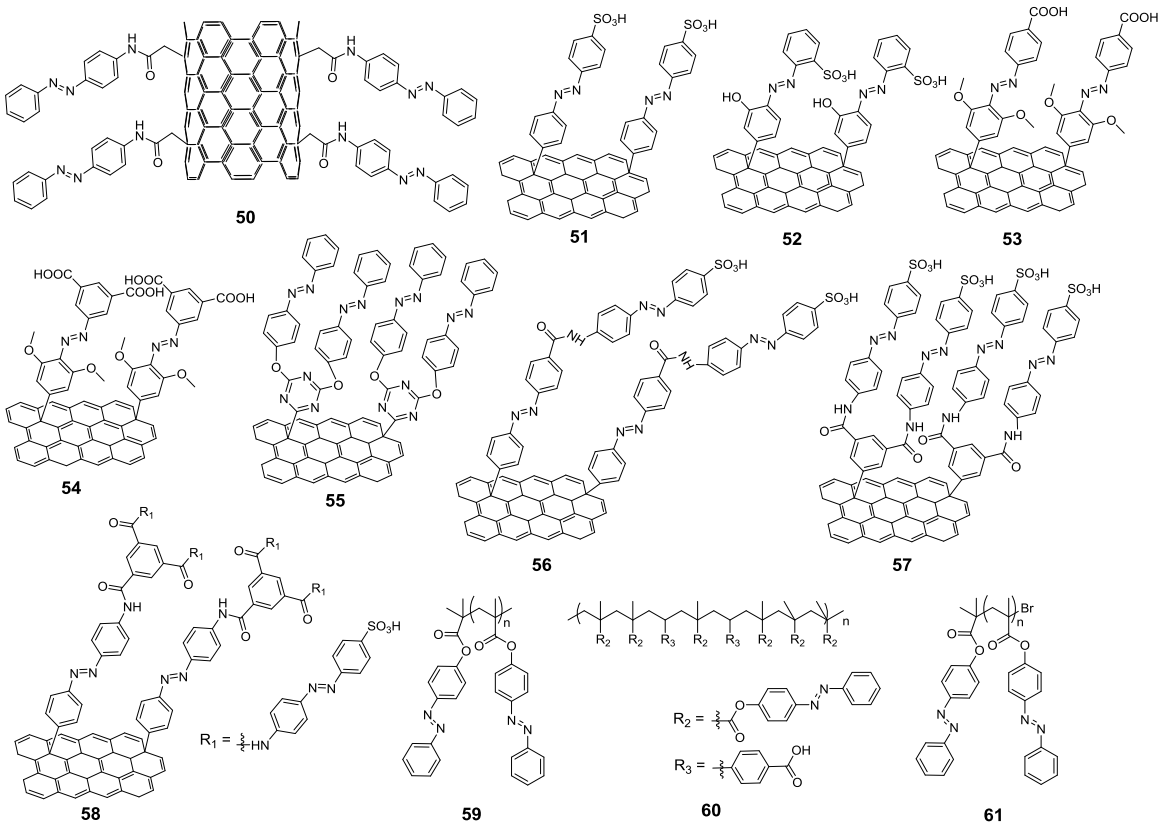

Figure 9. Example of azobenzene derivatives on SWCNT, RGO or poly(methacrylate), PMA supports for controlling intermolecular packing.

Table 3 Reported energy densities and half-lifes of the *cis* isomer of azobenzenes covalently bound to carbon support (SWCNT and RGO) or polymer matrix.

	support	ED, kJ/kg	$t_{1/2}$, h (25 °C)
Azobenzene	--	270	1.4
50[79]	SWCNT	202	33
51[80]	RGO	270	116
52[80]	RGO	150	5408
53[81]	RGO	403	792
54[82]	RGO	497*	1248
55[83]	RGO	288**	1320
56[84]	RGO	346	1120
57[84]	RGO	472	900
58[85]	RGO	540	1250
59[86]	PMA	104	55
60[87]	PMA	90	75
61[88]	PMA	510±115^	76

* The lack of cited heating rate precludes independent calculation of ED from the shown DSC trace, but the claimed ED requires an implausibly high ΔH_{isom} of ~300 kJ/(mol azobenzene) based on the reported grafting density of 1/17 and assuming pure graphene as support. ΔH_{isom} ~300 kJ/(mol azobenzene) corresponds to >80% of the absorbed photon energy converted to ΔH_{isom}, which is unprecedented.

** The number shown appears in the text of ref. [83]; our calculations using data in Fig. 5a-b (cited by the authors in support of this ED) gives ED <115 kJ/mol.

^ The value is derived from DSC traces that correspond to negative heat capacity: in the shown traces the temperature decreases while the material is heated.

All ED values reported in this review (or the cited literature) refer to neat isomers, irrespectively of how technically feasible it is to photoisomerize bulk samples of highly absorbing powders or how to discharge such a battery given the poor thermal conductivity of these powders. Azobenzene-derivatized polymers [86-88] may be deployed as free-standing films but most molecules considered to date will probably have to be used as solutions or deposited on supports, further reducing the device ED. Hence, some effort has been devoted to turn at least one isomer in a pair into a room-temperature liquid by peripheral substitution. While this approach invariably reduces the ED of the neat material, under what circumstances it would maximize device ED, or what rheological properties such liquids need to satisfy to enable device manufacture and operation has not yet been discussed in the literature.

Perhaps the most successful implementation of this approach are NBD derivatives **62**-**67**[89] (Figure 10), which are both liquid at room temperature and absorb the high-energy tail of solar radiation. Energy density of up to 577 kJ/kg was claimed, but it should be noted that reported ΔH_{isom} for **62** (152 kJ/mol) is unprecedented, being 35% higher than that of unsubstituted NBD, over 3 times that of structurally analogous **65** and twice the DFT value calculated by the authors. ΔH_{isom} of all other derivatives of NBD suggest at most modest dependence of isomerization thermodynamics on substituents (all reported experimental values are in the ~100 - ~50 kJ/(mol NBD) range). The original report acknowledged that estimated ΔH_{isom} for **62** was atypical but its origin remains unknown. We speculate that the 3-fold difference in ΔH_{isom} for structurally analogous **62** and **65** suggests the potential uncertainty of DSC measurements, from which the reported ΔH_{isom} values were estimated. Consequently, we suggest that until further validation, derivative **62** should be assumed to have ΔH_{isom} similar to that of unsubstituted NBD.

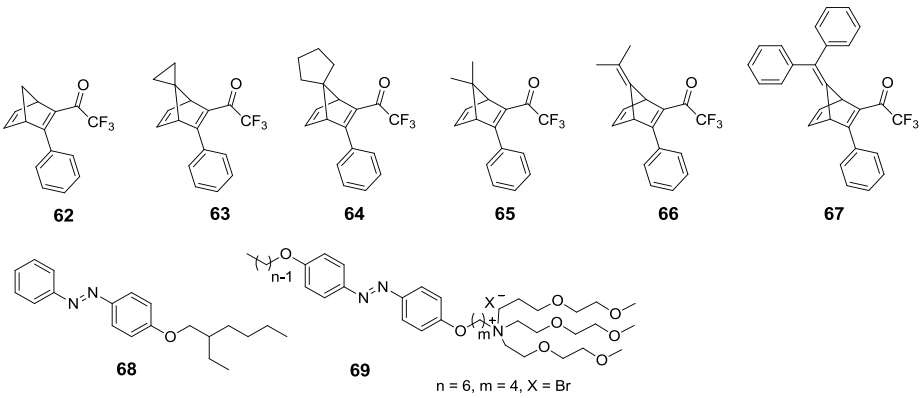

Figure 10 NBD/QC and azobenzene derivatives with at least one isomer being liquid at room temperature.

A single alkoxy substituent turns azobenzene into a room-temperature liquid (**68**) without affecting estimated ΔH_{isom} (52 kJ/mol vs. 49 kJ/mol for unsubstituted azobenzene) but approximately halving the maximum achievable ED (169 kJ/kg vs. 270 kJ/kg) due to the extra mass.[90] The *trans* isomer of derivative **69** is a solid but the *cis* analog is a liquid, with the latent heat of phase change increasing ΔH_{isom} to 97.1 kJ/mol, although the additional mass reduced ED to only 128 kJ/kg,[91] or less than half that of unsubstituted azobenzene. It seems plausible that these EDs can be increased by further optimizations of the substitution patterns.

3.2. Self-discharge rate

A major advantage of molecular solar thermal energy storage over the thermophysical analog is its insensitivity to thermal insulation because it stores free energy not as a thermal gradient but as excess chemical potential of a metastable molecule. Consequently, the shelf life of a molecular solar thermal battery is determined by the storage temperature and kinetic stability of the metastable isomer, i.e., the activation barrier of the exothermic reaction, $\Delta G_{rev}^{\neq}$. For example, according to the Eyring equation, a battery based on a reaction with $\Delta G_{rev}^{\neq}$ = 125 kJ/mol will self-discharge by half (i.e., lose

half of its free energy) in ~12 years at 25 °C, which is comparable or better than many batteries in commercial use now. The lower limit of $\Delta G_{rev}^{\neq}$ is determined by its intended application and storage temperature. For example a molecular solar thermal battery designed to provide nighttime ambient heating by capturing and storing a fraction of daytime sunlight will probably operate adequately with $\Delta G_{rev}^{\neq}$ = 100 kJ/mol. At smaller barriers for thermal relaxation of the metastable isomer will likely compete with its generation by photoisomerization, making $\Delta G_{rev}^{\neq}$ < 100 kJ/mol undesirable. In other words, practical molecular solar thermal solar energy storage requires exothermic reactions with $\Delta G_{rev}^{\neq}$ in the 100 – 125 kJ/mol range.[4]

With the exception of azobenzene, the reactions in Table 1 have $\Delta G_{rev}^{\neq}$ in this range or higher, albeit most with suboptimal ΔG_{isom}. Increasing ΔG_{isom} typically decreases $\Delta G_{rev}^{\neq}$ so that the self-discharge rate is still an important consideration in optimizing the molecular design of material for molecular solar thermal energy storage. Few examples of ordered azobenzene materials that increased simultaneously ΔG_{isom} and $\Delta G_{rev}^{\neq}$ compared to the Table 1 baseline have been claimed[27] but given the technical difficulties of accurate kinetic and thermodynamic characterization of such materials it is probably prudent to view these claims at tentative for now.

3.3. Energy conversion efficiency

Only a fraction of the energy of absorbed photon can be converted into ΔG_{isom}: the upper limit is determined by the features of the energy surface (Figure 1) and is approximately the ratio of ΔG_{isom} (or ΔH_{isom}) and the energy of the absorbed photon, i.e., $\lambda_{abs}\Delta G_{isom}/(N_A hc)$, where N_A is the Avogadro's number, h is Planck's constant and c is the speed of light. Quantum yields of isomerization $\varphi_{isom} < 1$ and absorbing metastable isomers reduce the fraction of the solar energy absorbed by a macroscopic sample that is converted to ΔG_{isom} below the number determined by the energy surface. For example, the energy difference between unsubstituted NBD and QC is ~20% of the energy difference between S_0 NBD and the corresponding S_1 Frank-Condon structure, which determines the minimum energy of the photon that causes photoisomerization (neglecting vibronic effects). However, because only 5% of molecules excited to the S_1 Frank-Condon structure relax to QC, the NBD/QC pair converts <1% of absorbed energy into chemical potential, with the rest heating the material and its surroundings. In theory, local heating resulting from this dissipated photon energy increases the population of vibrationally excited chromophores, which, depending on the topologies of the S_0 and S_1 surfaces in the vicinity of the stable isomer and its Frank-Condon geometry may allow absorption of lower-frequency photons or (probably minor) increases in the quantum yields. This presently-speculative scenario would increase the average fraction of the photon energy converted to chemical potential.

Several definitions of energy conversion efficiency (η) have appeared in the literature on molecular solar thermal energy storage,[46, 47, 54, 79] but the simplest one is the fraction of absorbed energy converted into ΔG_{isom}. This value decreases as the battery approaches full charge for any molecular solar thermal energy battery that uses an absorbing metastable isomer. At constant radiative flux, lower efficiency leads to longer charging times and higher thermal fluxes that may require active cooling. All other factors being constant, the efficiency increases with ΔG_{isom}, the difference in absorptivities of the two isomers at irradiation wavelengths and both absolute quantum yield of the productive isomerization and its ratio to that of unproductive isomerization.

Energy conversion efficiency of molecular solar thermal storage has attracted relatively little attention[46, 47, 54, 79] because it is less significant in determining the utility and application niches of this storage method compared to energy and power densities, and spectral overlap. One area where the thermodynamic limits to the energy conversion efficiency have been discussed[92, 93] is to justify the potential role of molecular solar thermal energy storage in the technological mix for utilizing solar energy. The argument is that if solar batteries have attainable energy conversion efficiencies similar to that for photovoltaic cells, they are more likely to be perceived as potentially useful.[94]

4. Release of energy

The exothermic reaction from metastable isomer of the photoswitch back to the stable isomer discharges the solar thermal battery, with the process characterized by the achievable power density and discharge temperature. The two are related and the discharge temperature may be limited by tolerance for side reactions during discharge, whose probability generally increases with temperature. We are not aware of studies that aimed specifically at optimizing the molecular geometry to maximize achievable power density or discharge temperature but a model to do so, using the standard and activation free energies of isomerization and device geometry was reported.[95]

4.1. Power density

The average power density, PD, under isothermal discharge is related to the energy density, ED, of a fully charged battery as[4]

$$\mathrm{PD}_{1\to\chi} = -\frac{\chi \mathrm{ED}}{\ln(1-\chi)}\frac{k_B T}{h} e^{-\Delta H_{rev}^{\neq}/RT + \Delta S_{rev}^{\neq}/R}$$

where χ is the extent of the battery discharge (in fully charged battery χ=0), $\Delta H_{rev}^{\neq}$ and $\Delta S_{rev}^{\neq}$ are the activation enthalpy and entropy of isomerization of the metastable isomer (often $\Delta S_{rev}^{\neq} \sim 0$), *T* is the discharge temperature, and k_B, *h* and *R* are the Boltzmann, Planck and gas constants, respectively. The power density is highest at the beginning of discharge of a fully charged battery and decreases as the fraction of the metastable isomer decreases. Higher temperatures lead to higher power densities because they correspond to faster isomerization. If the battery does not allow isothermal discharge, for example because of the limited thermal conductivity of the photoactive material, achievable PD is likely to be lower than the equation above predicts. A battery with ED = 1 MJ/kg and $\Delta G_{rev}^{\neq}$ = 125 kJ/mol has the maximum power density of ~2 mW/kg at room temperature (corresponding to self-discharge) and ~400 W/kg at 100 °C. In comparison, the maximum achievable power densities of batteries in commercial use now are 50 – 5000 W/kg.

4.2. Discharge triggers

Because temperature increases reaction rate, battery discharge can be self-sustaining if a fraction of the released heat is used to maintain the temperature of the material at a value corresponding to the reaction rate that gives the desired power output. Likewise, stopping the discharge simply requires allowing its temperature to drop below a threshold. Consequently, a discharge can be initiated by localized transient heating,[79, 85] or another form of energy input that accelerates the exothermic reaction, such as localized photoirradiation[81, 85] or application of electrostatic potential.[96, 97] Alternatively, the metastable isomer can be exposed to a catalyst. Several transition metal complexes effectively catalyse the QC->NBD conversion. A common reaction mechanism requires insertion of a metal atom into a strained C-C bond of QC, followed by concerted reductive elimination or a two-step elimination via a carbocation.[21] A proposed mechanism for cobalt-phthalocyanine (CoPc) example is shown in Figure 11 in which is used for the reaction from **70** to **11**.[49] Potential catalysts for $FvRu_2$ isomerization include ligands for Ru and metal-based one-electron oxidants or Lewis acids, $AgNO_3$ being currently the most efficient.[39, 98] For the VHF->DHA reversion, Lewis acids such as $[Cu(CH_3CN)_4]BF_4$ are efficient.[36, 99] [36, 39, 49, 98, 99] Practical implementations of catalytic discharge presents numerous challenges,[100, 101] which remain to be systematically addressed. Optimal solutions for triggering discharge has attracted little attention.

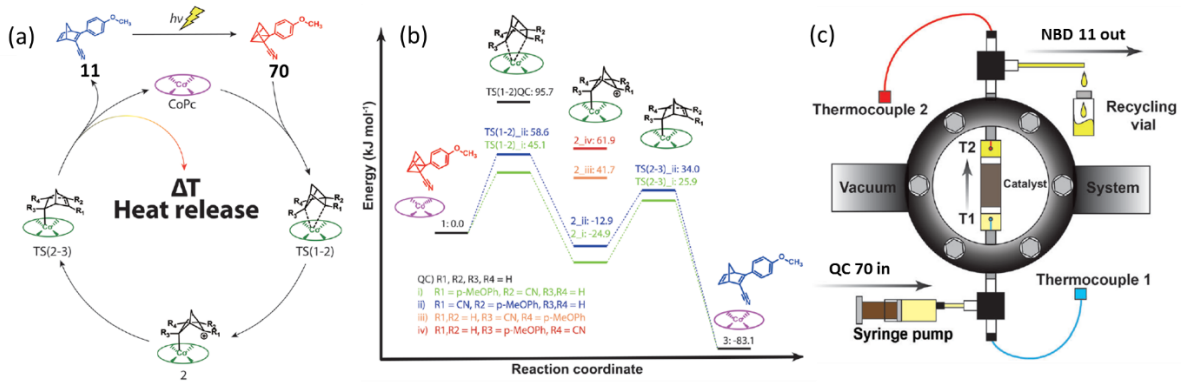

*Figure 11. Catalytic isomerization of QC **70** to NBD **11** by cobalt-phthalocyanine (CoPc): (a) The proposed catalytic cycle. (b) The corresponding energy diagram at the M06/6-31+G* level of DFT with a PCM model of the solvent. The green bars correspond to the lowest-energy reaction path. (c) A device used to demonstrate heat release accompanying catalyst isomerizatin. The catalyst (CoPc) was physisorbed on an activated carbon support through which a solution of QC **70** was pumped; the whole assembly was placed in a high vacuum chamber. Reproduced with persmission from Ref. [49]. Copyright (2019) The Royal Society of Chemistry.*

5. Summary and outlook

Developing practical solutions for molecular solar thermal energy storage presents a range of challenges encompassing synthetic and physical chemistry (e.g., the effect of molecular strain on quantum yields), material science (e.g., rheological and thermomechanical properties of the photoactive material) and device engineering (e.g., heat management during charging and discharging). It seems likely that specific molecules have to be designed for each possible deployment niche, because distinct applications assign different relative values to individual performance characteristics (energy and power densities, accessible discharge temperature, cyclability, self-discharge rate) and it seems very unlikely that these distinct demands can ever be met by a single molecule or even a single reaction. For example, maximizing the energy density is likely to be much more important for batteries intended for mobile rather than stationary applications, while self-discharge rate may determine suitability of specific chemistry for use in emergency power supplies in remote locations. Acceptable power densities and discharge temperatures are different if molecular solar thermal battery is used for ambient heating or to generate electric power.

Contemporary research in molecular solar thermal energy storage focuses primarily on acquiring empirical chemical data from which usefully generalizable trends relating molecular structure, photophysics, isomerization kinetics and thermodynamics, and synthetic accessibility may emerge. Such work has been largely confined to the four reactions in Table 1 but the data available to date does not obviously establish that this reaction set is the most likely source of chemistries to enable practical molecular solar thermal energy storage. Such storage imposes considerable specific demands on suitable reactions and molecules. Yet, the ever-expanding universe of molecular photoswitches seems very likely to offer new candidates with chemical and physical attributes that are at least as well suited for molecular solar thermal energy storage as the 4 reactions underlying the vast majority of contemporary work in the field. We are not aware of any systematic effort to assess the existing diverse set of photoswitches for their applicability as molecular solar thermal batteries, for example computationally.

Further progress in the field will likely depend on defining more precisely, quantitatively and generally (1) the fundamental limits that determine the relationship among ΔG_{isom}, $\Delta G_{rev}^{\neq}$, φ_{isom} and the photoisomerization wavelength, and their dependence on the molecular structure and (2) the range of the values of these parameters compatible with practically useful implementations of molecular solar thermal solar energy storage. The first task is of fundamental significance and is worth pursuing regardless of the prospect of molecular solar thermal energy storage. Conversely, the second task cannot be pursued meaningfully without first defining the intended application niche, which limits the

range of possible engineering implementations of each stage of battery operation (i.e., charge, storage, discharge), which constraints the chemistry (ΔG_{isom}, $\Delta G_{rev}^{\neq}$, φ_{isom} and the photoisomerization wavelength) and the material properties (e.g., phase, thermal conductivity, rheology) of the active component. Only a small fraction of the reported studies in molecular solar thermal energy storage attempt to take such a systems approach, reflecting the practical challenges of conducting such multidisciplinary investigations.

Acknowledgment. This work was supported by the EPSRC Early Career Award (EP/L000075/1) and ACS PRF (58885-ND7)

Keywords: molecular solar thermal, photoisomerization, photoswitch, solar energy storage, strain energy

6. References

[1] Renewables 2018. *International Energy Agency*. **2018**: www.iea.org/renewables 2018.
[2] E. Kabir, P. Kumar, S. Kumar, A. A. Adelodun, K.-H. Kim *Renew. Sustain. Energy. Rev.* **2018**, *82*, 894-900.
[3] Y. Tachibana, L. Vayssieres, J. R. Durrant *Nat. Photonics*. **2012**, *6*, 511-518.
[4] T. J. Kucharski, Y. Tian, S. Akbulatov, R. Boulatov *Energy Environ. Sci.* **2011**, *4*, 4449-4472.
[5] I. Gur, K. Sawyer, R. Prasher *Science*. **2012**, *335*, 1454-1455.
[6] H. M. Bandara, S. C. Burdette *Chem. Soc. Rev.* **2012**, *41*, 1809-1825.
[7] D. H. Waldeck *Chem. Rev.* **1991**, *91*, 415-436.
[8] A. D. Dubonosov, V. A. Bren, V. A. Chernoivanov *Russ. Chem. Rev.* **2002**, *71*, 917-927.
[9] M. Irie, T. Fukaminato, K. Matsuda, S. Kobatake *Chem. Rev.* **2014**, *114*, 12174-12277.
[10] G. Berkovic, V. Krongauz, V. Weiss *Chem. Rev.* **2000**, *100*, 1741−1753.
[11] S. L. Broman, M. B. Nielsen *Phys. Chem. Chem. Phys.* **2014**, *16*, 21172-21182.
[12] H. Bouas-Laurent, A. Castellan, J.-P. Desvergne, R. Lapouyade *Chem. Soc. Rev.* **2000**, *29*, 43-55.
[13] J.-F. Xu, Y.-Z. Chen, L.-Z. Wu, C.-H. Tung, Q.-Z. Yang *Org. Lett.* **2013**, *15*, 6148–6151.
[14] H. Nakai, K. Isobe *Coord. Chem. Rev*. **2010**, *254*, 2652-2662.
[15] J. S. Splitter, M. Calvin *J. Org. Chem.* **1958**, *23*, 651.
[16] In their paper "Energy-Storage in Organic Photoisomers" published in *J. Photochem*. **1979**, 10, 1-18, Jones, Chiang, and Xuan, P. T. wrote "The potential for storage of radiant energy in chemical bonds was recognized as early as 1909". A similar claim of early origins of the idea of solar thermal energy storage has since found its way in a few research papers and reviews in the field, but we question how plausible such a claim is. Jones et al. supported their assertion by citing a Chemical Abstracts (CA) entry of a paper by Weigert, F in Jahrbuch für Photographie, Kinematographie und Reproduktionsverfahren **1909**, 109. While we were unable to locate the text of this paper, the cited CA entry reads: "From experiments on the polymerization of anthracene in toluene to dianthracene, the author concludes that at least 15% of the energy of light can be converted into available mechanical energy, without the intervention of plant life." This statement hardly suggests solar thermal energy storage. Furthermore, in a preceding paper (Berichte der Deutschen Chemischen Gesellschaft **1909**, 42, 850-862) Weigert claimed (again, according to the CA): "From experiments at 85° and 105° the equilibrium constant in the dark [of anthracene dimerization] is shown to increase with increasing temp." Such a dependence would render anthracene dimer rather unsuitable for solar thermal energy storage. We now know that anthracene cannot be dimerized thermally, suggesting that the reaction whose thermal equilibrium Weigert measured was not anthracene dimerization.
[17] L. Anders, K. Moth-Poulsen in *Molecular Solar-Thermal Energy Storage: Molecular Design and Functional Devices,* (Eds.: H. Tian, G. Boschloo, A. Hagfeldt), Springer, Singapore, **2018**, pp.327-352.
[18] A. Lennartson, A. Roffey, K. Moth-Poulsen *Tetrahedron Lett.* **2015**, *56*, 1457-1465.
[19] L. Dong, Y. Feng, L. Wang, W. Feng *Chem. Soc. Rev.* **2018**, *47*, 7339-7368.
[20] X. Zhang, L. Hou, P. Samori *Nat. Commun.* **2016**, *7*, 11118.
[21] V. A. Bren', A. D. Dubonosov, V. I. Minkin, V. A. Chernoivanov *Russ. Chem. Rev.* **1991**, *60*, 451-469.
[22] X.-w. An, Y.-d. Xie *Thermochimi. Acta*. **1993**, *220*, 17-25.

[23] H. M. Frey *J. Chem. Soc.* **1964**, 365-367.
[24] V. Gray, A. Lennartson, P. Ratanalert, K. Borjesson, K. Moth-Poulsen *Chem. Commun.* **2014**, *50*, 5330-5332.
[25] W. Fuß, K. K. Pushpa, W. E. Schmida, S. A. Trushin *Photochem. Photobiol. Sci.* **2002**, *1*, 60-66.
[26] A. W. Adamson, A. Vogler, H. Kunkely, R. Wachter *J. Am. Chem. Soc.* **1978**, *100*, 1298-1300.
[27] A. M. Kolpak, J. C. Grossman *Nano Lett.* **2011**, *11*, 3156-3162.
[28] S. L. Broman, S. L. Brand, C. R. Parker, M. Å. Petersen, C. G. Tortzen, A. Kadziola, K. Kilså, M. B. Nielsen *ARKIVOC*. **2011**, *ix*, 51-67.
[29] H. Gorner, C. Fischer, S. Gierisch, J. Daub *J. Phys. Chem.* **1993**, *97*, 4110-4117.
[30] S. T. Olsen, J. Elm, F. E. Storm, A. N. Gejl, A. S. Hansen, M. H. Hansen, J. R. Nikolajsen, M. B. Nielsen, H. G. Kjaergaard, K. V. Mikkelsen *J. Phys. Chem. A*. **2015**, *119*, 896-904.
[31] M. H. Hansen, J. Elm, S. T. Olsen, A. N. Gejl, F. E. Storm, B. N. Frandsen, A. B. Skov, M. B. Nielsen, H. G. Kjaergaard, K. V. Mikkelsen *J. Phys. Chem. A*. **2016**, *120*, 9782-9793.
[32] R. Boese, J. K. Cammack, A. J. Matzger, K. Pflug, W. B. Tolman, K. P. C. Vollhardt, T. W. Weidman *J. Am. Chem. Soc.* **1997**, *119*, 6757-6773.
[33] Y. Kanai, V. Srinivasan, S. K. Meier, K. P. Vollhardt, J. C. Grossman *Angew. Chem. Int. Ed.* **2010**, *49*, 8926-8929.
[34] Y. Norikane, R. Katoh, N. Tamaoki *Chem. Commun.* **2008**, 1898-1900.
[35] R. Siewertsen, H. Neumann, B. Buchheim-Stehn, R. Herges, C. Nather, F. Renth, F. Temps *J. Am. Chem. Soc.* **2009**, *131*, 15594-15595.
[36] Z. Wang, J. Udmark, K. Borjesson, R. Rodrigues, A. Roffey, M. Abrahamsson, M. B. Nielsen, K. Moth-Poulsen *ChemSusChem*. **2017**, *10*, 3049-3055.
[37] M. R. Harpham, S. C. Nguyen, Z. Hou, J. C. Grossman, C. B. Harris, M. W. Mara, A. B. Stickrath, Y. Kanai, A. M. Kolpak, D. Lee, D. J. Liu, J. P. Lomont, K. Moth-Poulsen, N. Vinokurov, L. X. Chen, K. P. Vollhardt *Angew. Chem. Int. Ed.* **2012**, *51*, 7692-7696.
[38] K. Börjesson, A. Lennartson, K. Moth-Poulsen *J. Fluor. Chem.* **2014**, *161*, 24-28.
[39] K. Borjesson, D. Coso, V. Gray, J. C. Grossman, J. Guan, C. B. Harris, N. Hertkorn, Z. Hou, Y. Kanai, D. Lee, J. P. Lomont, A. Majumdar, S. K. Meier, K. Moth-Poulsen, R. L. Myrabo, S. C. Nguyen, R. A. Segalman, V. Srinivasan, W. B. Tolman, N. Vinokurov, K. P. Vollhardt, T. W. Weidman *Chem. Eur. J.* **2014**, *20*, 15587-15604.
[40] A. Lennartson, A. Lundin, K. Borjesson, V. Gray, K. Moth-Poulsen *Dalton Trans.* **2016**, *45*, 8740-8744.
[41] K. Börjesson, D. Dzebo, B. Albinsson, K. Moth-Poulsen *J. Mater. Chem. A*. **2013**, *1*, 8521-8524.
[42] A. International in Standard Tables for Reference Solar Spectral Irradiances: Direct Normal and Hemispherical on 37° Tilted Surface, West Conshohocken, PA, **2012**, DOI: 10.1520/g0173-03r12.
[43] A. Lennartson, M. Quant, K. Moth-Poulsen *Synlett*. **2015**, *26*, 1501-1504.
[44] M. Quant, A. Lennartson, A. Dreos, M. Kuisma, P. Erhart, K. Borjesson, K. Moth-Poulsen *Chem. Eur. J.* **2016**, *22*, 13265-13274.
[45] M. J. Kuisma, A. M. Lundin, K. Moth-Poulsen, P. Hyldgaard, P. Erhart *J. Phys. Chem. C*. **2016**, *120*, 3635-3645.
[46] M. Kuisma, A. Lundin, K. Moth-Poulsen, P. Hyldgaard, P. Erhart *ChemSusChem*. **2016**, *9*, 1786-1794.
[47] K. Jorner, A. Dreos, R. Emanuelsson, O. El Bakouri, I. Fdez. Galván, K. Börjesson, F. Feixas, R. Lindh, B. Zietz, K. Moth-Poulsen, H. Ottosson *J. Mater. Chem. A*. **2017**, *5*, 12369-12378.
[48] M. Jevric, A. U. Petersen, M. Manso, S. Kumar Singh, Z. Wang, A. Dreos, C. Sumby, M. B. Nielsen, K. Borjesson, P. Erhart, K. Moth-Poulsen *Chem. Eur. J.* **2018**, *24*, 12767-12772.
[49] Z. Wang, A. Roffey, R. Losantos, A. Lennartson, M. Jevric, A. U. Petersen, M. Quant, A. Dreos, X. Wen, D. Sampedro, K. Börjesson, K. Moth-Poulsen *Energy Environ. Sci.* **2019**, *12*, 187-193.
[50] M. Manso, A. U. Petersen, Z. Wang, P. Erhart, M. B. Nielsen, K. Moth-Poulsen *Nat. Commun.* **2018**, *9*, 1945.

[51] M. Manso, B. E. Tebikachew, K. Moth-Poulsen, M. B. Nielsen *Org. Biomol. Chem.* **2018**, *16*, 5585-5590.
[52] M. Cacciarini, A. B. Skov, M. Jevric, A. S. Hansen, J. Elm, H. G. Kjaergaard, K. V. Mikkelsen, M. B. Nielsen *Chem. Eur. J.* **2015**, *21*, 7454-7461.
[53] A. B. Skov, S. L. Broman, A. S. Gertsen, J. Elm, M. Jevric, M. Cacciarini, A. Kadziola, K. V. Mikkelsen, M. B. Nielsen *Chem. Eur. J.* **2016**, *22*, 14567-14575.
[54] A. Dreos, K. Börjesson, Z. Wang, A. Roffey, Z. Norwood, D. Kushnir, K. Moth-Poulsen *Energy Environ. Sci.* **2017**, *10*, 728-734.
[55] X. Liu, Z. Xu, J. M. Cole *J. Phys. Chem. C*. **2013**, *117*, 16584-16595.
[56] A. K. Saydjari, P. Weis, S. Wu *Adv. Energy Mater.* **2017**, *7*, 1601622.
[57] Z. Huang, Q.-Z. Yang, D. Khvostichenko, T. J. Kucharski, J. Chen, R. Boulatov *J. Am. Chem. Soc.* **2009**, *131*, 1407-1409.
[58] H. Nakai, M. Inamori, Y. Ikabata, Q. Wang *J. Phys. Chem. A*. **2018**, *122*, 8905-8910.
[59] Q.-Z. Yang, Z. Huang, T. J. Kucharski, D. Khvostichenko, J. Chen, R. Boulatov *Nat. Nanotechnol.* **2009**, *4*, 302-306.
[60] T. J. Kucharski, Z. Huang, Q.-Z. Yang, Y. Tian, N. C. Rubin, C. D. Concepcion, R. Boulatov *Angew. Chem. Int. Ed.* **2009**, *48*, 7040-7043.
[61] T. J. Kucharski, Q.-Z. Yang, Y. Tian, R. Boulatov *J. Phys. Chem. Lett.* **2010**, *1*, 2820-2825.
[62] S. Akbulatov, Y. Tian, R. Boulatov *J. Am. Chem. Soc.* **2012**, *134*, 7620-7623.
[63] S. Akbulatov, Y. Tian, E. Kapustin, R. Boulatov *Angew. Chem. Int. Ed.* **2013**, *52*, 6992-6995.
[64] S. Akbulatov, Y. Tian, Z. Huang, T. J. Kucharski, Q.-Z. Yang, R. Boulatov *Science*. **2017**, *357*, 299-303.
[65] Y. Tian, T. J. Kucharski, Q.-Z. Yang, R. Boulatov *Nat. Commun.* **2013**, *4*, 2538.
[66] Z. Huang, Q.-Z. Yang, T. J. Kucharski, D. Khvostichenko, S. M. Wakeman, R. Boulatov *Chem. Eur. J.* **2009**, *15*, 5212-5214.
[67] Y. Wang, Y. Tian, Y. Chen, L. Niu, L. Wu, C. Tung, Q. Yang, R. Boulatov *Chem. Commun.* **2018**, *54*, 7991-7994.
[68] Z. S. Kean, S. Akbulatov, Y. Tian, R. A. Widenhoefer, R. Boulatov, S. L. Craig *Angew. Chem., Int. Ed.* **2014**, *52*, 14508-14511.
[69] E. Durgun, J. C. Grossman *J. Phys. Chem. Lett.* **2013**, *4*, 854-860.
[70] Y. Tian, R. Boulatov *Phys. Chem. Chem. Phys*. **2016**, *18*, 26990-26993.
[71] A. Vlasceanu, S. L. Broman, A. S. Hansen, A. B. Skov, M. Cacciarini, A. Kadziola, H. G. Kjaergaard, K. V. Mikkelsen, M. B. Nielsen *Chem. Eur. J.* **2016**, *22*, 10796-10800.
[72] A. Vlasceanu, B. N. Frandsen, A. B. Skov, A. S. Hansen, M. G. Rasmussen, H. G. Kjaergaard, K. V. Mikkelsen, M. B. Nielsen *J. Org. Chem.* **2017**, *82*, 10398-10407.
[73] Z. Huang, R. Boulatov *Pure Appl. Chem.* **2010**, *82*, 931-951.
[74] L. Anderson, R. Boulatov *Adv. Phys. Org. Chem.* **2018**, *52*, 87-143.
[75] H. Zhang, X. Li, Y. Lin, F. Gao, Z. Tang, P. Su, W. Zhang, Y. Xu, W. Weng, R. Boulatov *Nat. Commun.* **2017**, *8*, 1147.
[76] J. Wang, T. Kouznetsova, R. Boulatov, S. Craig *Nat. Commun.* **2016**, *7*, 13433-13451.
[77] E. N. Cho, D. Zhitomirsky, G. G. Han, Y. Liu, J. C. Grossman *ACS Appl. Mater. Interfaces*. **2017**, *9*, 8679-8687.
[78] T. J. Kucharski, R. Boulatov *Fundamentals of molecular photoactuation* in *Optical Nano and Micro Actuator Technology CRC Press,* **2011**, pp.83-106.
[79] T. J. Kucharski, N. Ferralis, A. M. Kolpak, J. O. Zheng, D. G. Nocera, J. C. Grossman *Nat. Chem.* **2014**, *6*, 441-447.
[80] Y. Feng, H. Liu, W. Luo, E. Liu, N. Zhao, K. Yoshino, W. Feng *Sci. Rep.* **2013**, *3*, 3260.
[81] W. Luo, Y. Feng, C. Cao, M. Li, E. Liu, S. Li, C. Qin, W. Hu, W. Feng *J. Mater. Chem. A*. **2015**, *3*, 11787-11795.
[82] W. Luo, Y. Feng, C. Qin, M. Li, S. Li, C. Cao, P. Long, E. Liu, W. Hu, K. Yoshino, W. Feng *Nanoscale*. **2015**, *7*, 16214-16221.

[83] W. Feng, S. Li, M. Li, C. Qin, Y. Feng *J. Mater. Chem. A*. **2016**, *4*, 8020-8028.
[84] X. Zhao, Y. Feng, C. Qin, W. Yang, Q. Si, W. Feng *ChemSusChem*. **2017**, *10*, 1395-1404.
[85] W. Yang, Y. Feng, Q. Si, Q. Yan, P. Long, L. Dong, L. Fu, W. Feng *J. Mater. Chem. A*. **2019**, *7*, 97-106.
[86] D. Zhitomirsky, E. Cho, J. C. Grossman *Adv. Energy Mater.* **2016**, *6*, 1502006.
[87] D. Zhitomirsky, J. C. Grossman *ACS Appl. Mater. Interfaces*. **2016**, *8*, 26319-26325.
[88] S. P. Jeong, L. A. Renna, C. J. Boyle, H. S. Kwak, E. Harder, W. Damm, D. Venkataraman *Sci. Rep.* **2017**, *7*, 17773.
[89] A. Dreos, Z. Wang, J. Udmark, A. Ström, P. Erhart, K. Börjesson, M. B. Nielsen, K. Moth-Poulsen *Adv. Energy Mater.* **2018**, *8*, 1703401.
[90] K. Masutani, M. A. Morikawa, N. Kimizuka *Chem. Commun.* **2014**, *50*, 15803-15806.
[91] K. Ishiba, M. A. Morikawa, C. Chikara, T. Yamada, K. Iwase, M. Kawakita, N. Kimizuka *Angew. Chem. Int. Ed.* **2015**, *54*, 1532-1536.
[92] K. Börjesson, A. Lennartson, K. Moth-Poulsen *ACS Sustainable Chem. Eng.* **2013**, *1*, 585-590.
[93] D. A. Strubbe, J. C. Grossman *J. Phys.: Condens. Matter*. **2019**, *31*, 034002.
[94] W. Shockley, H. J. Queisser *J. Appl. Phys.* **1961**, *32*, 510-519.
[95] M. H. Hansen, S. T. Olsen, K. O. Sylvester-Hvid, K. V. Mikkelsen *Chemical Physics*. **2019**, *519*, 92-100.
[96] O. Brummel, D. Besold, T. Dopper, Y. Wu, S. Bochmann, F. Lazzari, F. Waidhas, U. Bauer, P. Bachmann, C. Papp, H. P. Steinruck, A. Gorling, J. Libuda, J. Bachmann *ChemSusChem*. **2016**, *9*, 1424-1432.
[97] O. Brummel, F. Waidhas, U. Bauer, Y. Wu, S. Bochmann, H. P. Steinruck, C. Papp, J. Bachmann, J. Libuda *J. Phys. Chem. Lett.* **2017**, *8*, 2819-2825.
[98] K. Moth-Poulsen, D. Ćoso, K. Börjesson, N. Vinokurov, S. K. Meier, A. Majumdar, K. P. C. Vollhardt, R. A. Segalman *Energy Environ. Sci.* **2012**, *5*, 8534-8537.
[99] M. Cacciarini, A. Vlasceanu, M. Jevric, M. B. Nielsen *Chem. Commun.* **2017**, *53*, 5874-5877.
[100] U. Bauer, S. Mohr, T. Dopper, P. Bachmann, F. Spath, F. Dull, M. Schwarz, O. Brummel, L. Fromm, U. Pinkert, A. Gorling, A. Hirsch, J. Bachmann, H. P. Steinruck, J. Libuda, C. Papp *Chem. Eur. J.* **2017**, *23*, 1613-1622.
[101] U. Bauer, L. Fromm, C. Weiß, P. Bachmann, F. Späth, F. Düll, J. Steinhauer, W. Hieringer, A. Görling, A. Hirsch, H. P. Steinrück, C. Papp *J. Phys. Chem. C*. **2019**, *123*, 7654-7664.

TOC graphics and entry

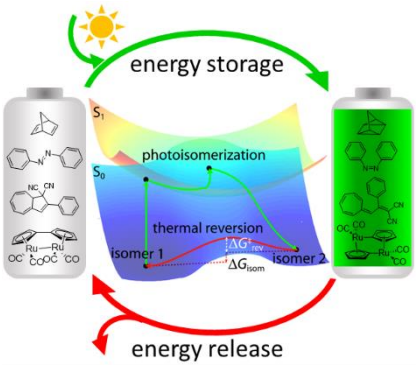

From light to heat through chemistry: A molecular photoswitch isomerizes when irradiated or heated. Photoswitches with a suitable energy profile provide a means of storing solar energy as metastable molecules in a thermodynamically closed operation, known as molecular solar thermal energy storage or a molecular solar thermal battery. This review assesses progress towards the deployment of molecular solar thermal energy storage based on empirical, computational or theoretical research published since 2011.

Biographies

 Cai-Li Sun received her Ph.D. from Technical Institute of Physics and Chemistry, Chinese Academy of Sciences (TIPC, CAS) in 2017 under the supervision of Prof. Chen-Ho Tung and Prof. Qing-Zheng Yang. She is currently a postdoctoral fellow in the group of Prof. Roman Boulatov at the University of Liverpool, UK. Her current reasearch focuses on photochemistry and mechanochemistry of supramolecular assemblies.

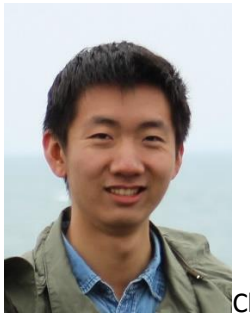 Chenxu Wang received his B.Eng. degree from Sichuan University, China in 2014 and M.Sc. degree from Loughborough University, UK in 2015. He is currently a graduate student at the University of Liverpool, UK supervised by Prof. Roman Boulatov, where he now is focused on polymer mechanochemistry.

 Roman Boulatov received his Ph.D. from Stanford University. After a postdoc at Harvard, he joined the University of Illinois, Urbana. During that time he developed a suite of experimental, theoretical and computational methods to explore, understand and exploit chemical reactions that occur when polymeric materials are subject to mechanical loads. He moved his group to the University of Liverpool in September 2012. His interests include the development and application of chemical tools to study macromolecular dynamics and response of soft matter to mechanical loads.